

# Synthesis and Luminescent Properties of Fluorene Copolymers Bearing DCM Pendants

Cheol Hong Cheon,<sup>†</sup> Sung-Hoon Joo,<sup>†</sup> Kyungkun Kim,<sup>†</sup> Jung-Il Jin,<sup>\*,†</sup> Hee-Won Shin,<sup>‡</sup> and Yong-Rok Kim<sup>†,‡</sup>

Division of Chemistry and Molecular Engineering and Center for Electro- and Photo-Responsive Molecules, Korea University, Seoul 136-701, Korea, and Department of Chemistry, Yonsei University, Seoul 120-749, Korea

Received October 5, 2004; Revised Manuscript Received May 24, 2005

**ABSTRACT:** A series of copolymers, poly[(9,9-dioctylfluorene-2,7-diyl)-*co*-(4-dicyanomethylene-2-methyl-6-[4-(diphenylamino)styryl]-4*H*-pyran-4',4''-diyl)], were synthesized by polymerizing 2,7-bis(4,4,5,5-tetramethyl-1,3,2-dioxaborolan-2-yl)-9,9-dioctylfluorene with mixtures of 2,7-dibromo-9,9-dioctylfluorene and 4-dicyanomethylene-2-methyl-6-[bis(4'-bromophenyl)amino]styryl]-4*H*-pyran (a DCM derivative) by the palladium-catalyzed Suzuki coupling reaction. The copolymers were characterized by molecular weight determination, elemental analysis, <sup>1</sup>H NMR, FT-IR spectroscopy, DSC, TGA, UV-vis spectroscopy, and photoluminescence (PL) and electroluminescence (EL) spectroscopy. The copolymers showed two absorption peaks at 380 and 485 nm, and the long-wavelength absorption increased with increasing the fraction of the DCM comonomer. The PL spectra of copolymers in chloroform solution displayed emission from both the main chain (420 nm) and DCM units (620 nm). In the solid state, however, PL spectra of copolymers showed only the long wavelength red emission at 620 nm with no trace of emission from the main chain, which implies a facile exciton migration or energy transfer to the lower energy sites from the fluorene part to the DCM part. This results in emission of only the red light originating from the latter segments. A study on time-resolved PL rise and decay of the polymers clearly supports the energy transfer mechanism. Light-emitting diode (LED) devices were fabricated to have the configuration of ITO (indium-tin oxide)/PEDOT/polymer/Li:Al alloy. EL spectra of the devices showed only red emissions as observed in the PL spectra of the polymers' thin films. EL efficiency decreased with increasing DCM contents. When a tris(8-hydroxyquinolato)aluminum (Alq<sub>3</sub>) layer was inserted between the emitting polymer layer and the cathode to make the ITO/PEDOT/polymer/Alq<sub>3</sub>/Li:Al alloy configuration, the device efficiencies became much higher (~10<sup>-2</sup>%) than those (5 × 10<sup>-5</sup>–5 × 10<sup>-3</sup>%) of single-layer devices.

## Introduction

Since the first report by the Cambridge group<sup>1</sup> on the electroluminescence (EL) of poly(*p*-phenylenevinylene) (PPV), enormous effort has been devoted to the synthesis of light-emitting,  $\pi$ -conjugated polymers because of their potential applications as emitting materials for electroluminescent displays.<sup>2–6</sup> Among the  $\pi$ -conjugated polymers, particularly a number of polyfluorene polymers and their derivatives have been attracting great of interest as very promising candidates for blue light-emitting diode (LED) materials because polyfluorenes (PFs) exhibit a high luminescence efficiency, good charge transport, excellent thermal and oxidative stability, tunability of physical properties through chemical modification and copolymerization, and good solubility in common organic solvents.<sup>7–9</sup> The major drawback<sup>8–15</sup> of PFs, however, is that they display a red-shifted and diminished emission upon thermal annealing or the passage of current. The source of this long wavelength emission was initially believed to be excimer emission from aggregates formed by  $\pi$ -stacking of the polymer chains.<sup>16</sup> Recently, the origin of the long wavelength emission, however, was ascribed to ketonic defects incorporated in the polymer backbone.<sup>17</sup> Various approaches have been adopted to suppress this undesired long wavelength emission: copolymerization with anthracene,<sup>18</sup> intro-

duction of a “kink” disorder along the conjugated polymer chain,<sup>13</sup> end-capping with a sterically hindered groups<sup>14</sup> or hole trapping moieties,<sup>15</sup> and introduction of bulky substituents at the 9-position of the fluorene unit.<sup>16a,19</sup>

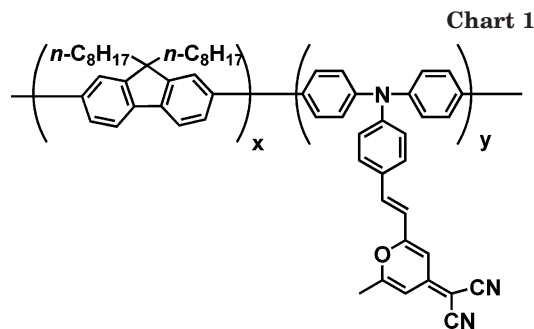
Meanwhile, attempts have been made to modify the structure of PFs which would favor an energy transfer from one part to the other in the molecules leading to changes in electronic properties. Very often this approach enables tunability of luminescent colors. One successful method is to dope the host PFs with a chromophore with desired luminescent properties.<sup>20</sup> The other method is copolymerization with low-band-gap comonomers.<sup>21–24</sup> Energy transfer and trapping of excitons or electrons between the chromophoric segments in conjugated polymer chains are known to be fast and efficient,<sup>21–23</sup> which shifts the wavelength of emitted light to a longer wavelength. Several groups studied fluorescence properties of the copolymers containing both the fluorene donor sites and other acceptor moieties.<sup>21–24</sup>

The blending approach has an advantage by which we can make a fine control of the nature and the amount of the incorporated dye. However, the blends usually suffer from long-term instability originating from the possible phase separation and aggregation formation. Direct incorporation of the low-band-gap comonomer units into polymer main chains appears to be an attractive strategy to overcome this drawback, although very often one has to go through a multistep synthetic route.

<sup>†</sup> Korea University.

<sup>‡</sup> Yonsei University.

\* Corresponding author. E-mail: jijin@korea.ac.kr.



In this investigation, we would like to report the preparation and luminescence properties of a series of dioctylfluorene copolymers containing moieties of the DCM structure well-known for red-light emission.<sup>25–27</sup> This article, in particular, discusses the synthesis of the new fluorene-based copolymers whose structures are shown above (Chart 1), energy transfer from the blue-light-emitting fluorene segments to the DCM units, and EL characteristics of LEDs fabricated from them. In the copolymers the DCM moieties are linked to the fluorene units through the triphenylamine (TPA) structure.

Among the three copolymers, PF-DCM 05 and PF-DCM 15 are of random sequence, whereas PF-DCM 50 is of alternating sequence (Chart 1). The numbers 05, 15, and 50 stand for the mole percent of the DCM monomer used in feed, respectively. Their actual compositions are described in the Results and Discussion.

## Experimental Section

**Materials.** Tetrahydrofuran (THF) was distilled over sodium/benzophenone.<sup>28</sup> Acetonitrile was distilled over  $P_2O_5$ . Dimethylformamide (DMF) was distilled over calcium hydride. Tetrakis(triphenylphosphine)palladium(0) was purchased from Strem Chemicals (Newburyport, MA) and was used as received. All other chemicals were purchased from Aldrich Chemical Co. (Milwaukee, WI), TCI (Tokyo, Japan), or Acros Chemicals (Geel, Belgium) and were used as received unless otherwise described. Poly(3,4-ethylenedioxythiophene) (PEDOT) doped with poly(styrenesulfonate) with an electrical conductivity of  $10 \text{ S cm}^{-1}$  was purchased from Aldrich Chemical Co. Tris(8-hydroxyquinolato)aluminum ( $Alq_3$ ) was purchased from TCI and used as received.

**Synthesis.** 2,7-Dibromo-9,9-dioctylfluorene (**1**)<sup>29</sup> and 2,7-bis(4,4,5,5-tetramethyl-1,3,2-dioxaborolan-2-yl)-9,9-dioctylfluorene (**2**)<sup>29</sup> were prepared according to the procedures reported in the literature, and 4-dicyanomethylene-2,6-dimethyl-4H-pyran (**3**) was synthesized from 2,6-dimethyl-4-pyrone as described by Woods.<sup>30</sup>

**4-[Bis(4'-bromophenyl)amino]benzaldehyde (4).** A 2.5 M *n*-butyllithium solution (4.6 mL,  $1.1 \times 10^{-2}$  mol) in hexane was added slowly to a solution of tris(4-bromophenyl)amine (5.0 g,  $1.1 \times 10^{-2}$  mol) in 30 mL of dry THF. After the reaction mixture was stirred at  $-78^\circ\text{C}$  for 1 h, 4.0 mL ( $5.2 \times 10^{-2}$  mol) of dimethylformamide (DMF) was added under a nitrogen atmosphere. The mixture was stirred for another 1 h and warmed to room temperature. After being kept for 1 h at room temperature, the reaction mixture was poured into distilled water. The aqueous solution was extracted with diethyl ether. The organic layer was separated and then dried over anhydrous magnesium sulfate. After removing the solvent, the product was purified by column chromatography on a silica gel column using a mixture of hexane/ethyl acetate = 1:15 (v/v) as an eluent. The product was green solid. Yield was 51% (2.3 g).  $^1\text{H NMR}$  (300 MHz,  $\text{CDCl}_3$ , ppm):  $\delta$  9.84 (s, 1H,  $-\text{CHO}$ ),  $\delta$  7.70 (d, 2H, Ar-H),  $\delta$  7.44 (d, 4H, Ar-H),  $\delta$  7.00 (m, 6H, Ar-H). Anal. Calcd for  $\text{C}_{19}\text{H}_{13}\text{BrNO}$ : C, 52.93; H, 3.04; N, 3.25%. Found: C, 52.81; H, 2.99; N, 3.29%.

**4-Dicyanomethylene-2-methyl-6-[[bis(4'-bromophenyl)amino]styryl]-4H-pyran (5).** A solution (50 mL) of com-

pound **4** (1.3 g,  $3.0 \times 10^{-3}$  mol) in acetonitrile was added dropwise to a mixture of compound **3** (2.6 g,  $1.5 \times 10^{-2}$  mol) and catalytic amount of piperidine in 150 mL of dry acetonitrile. After the reaction mixture was refluxed under a nitrogen atmosphere for 24 h, it was cooled to room temperature. After the solvent was removed by distillation, the crude product obtained was purified by column chromatography on a silica gel column using a mixture of hexane/ethyl acetate = 1:6 (v/v) as an eluent. The product was dark red solid. Yield was 47% (0.83 g).  $^1\text{H NMR}$  (300 MHz,  $\text{CDCl}_3$ , ppm):  $\delta$  7.42 (m, 7H, Ar-H and  $-\text{CH}=\text{}$ ),  $\delta$  7.00 (m, 6H, Ar-H),  $\delta$  6.65 (d, 1H, pyran-H),  $\delta$  6.54 (d, 1H,  $-\text{CH}=\text{}$ ),  $\delta$  6.52 (d, 1H, pyran-H),  $\delta$  2.4 (s, 3H,  $-\text{CH}_3$ ). Anal. Calcd for  $\text{C}_{29}\text{H}_{19}\text{Br}_2\text{N}_3\text{O}$ : C, 59.51; H, 3.27; N, 7.18%. Found: C, 59.62; H, 3.31; N, 7.20%.

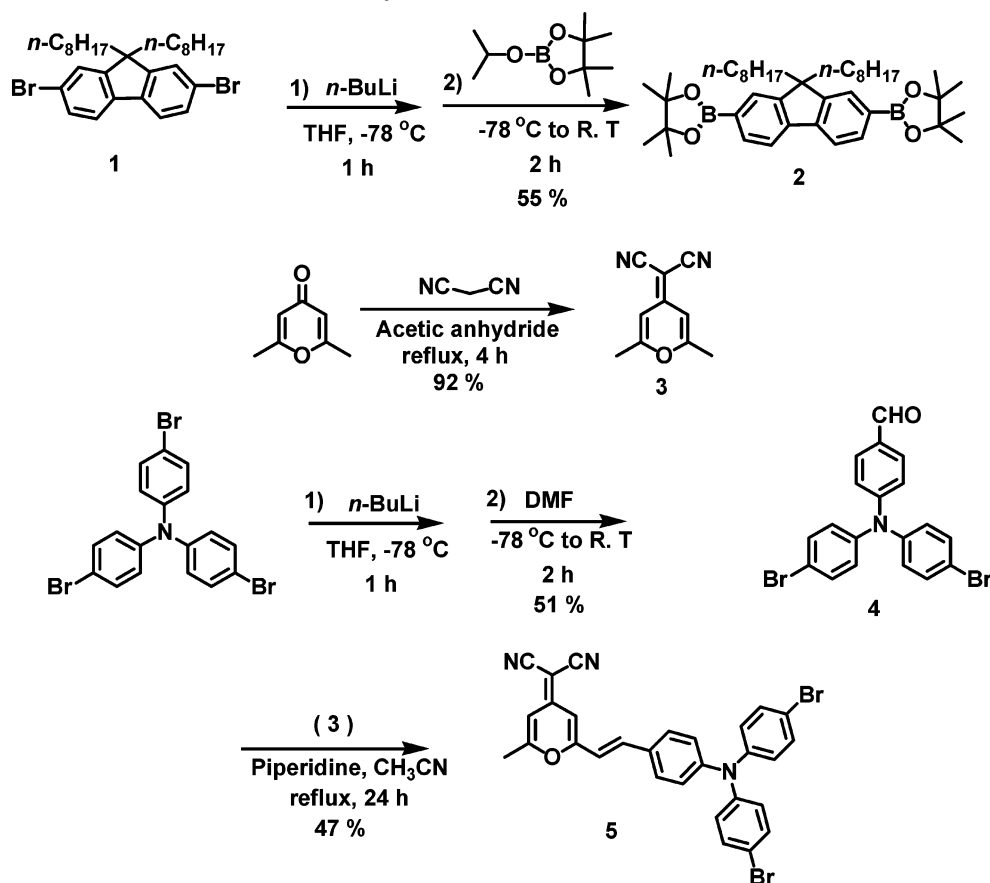
**Poly[2,7-(9,9-dioctylfluorene)] (PF).**<sup>31</sup> Poly[2,7-(9,9-dioctylfluorene)] (PF) was synthesized from a mixture of compounds **1** and **2** by the well-known palladium-catalyzed Suzuki coupling reaction according to the procedures reported in the literature.

**Poly[2,7-(9,9-dioctylfluorene)-co-(1,4-phenylene- $\{\beta$ -(2-(4-dicyanomethylene-6-methyl-4H-pyran)-yl)styryl)imino-1,4-phenylene] (PF-DCM 05).**<sup>31</sup> A mixture of compounds **1** (0.365 g,  $6.65 \times 10^{-4}$  mol), **2** (0.474 g,  $7.37 \times 10^{-4}$  mol), and **5** (0.043 g,  $7.37 \times 10^{-5}$  mol) and tetrakis(triphenylphosphine)palladium (8.5 mg,  $7.37 \times 10^{-6}$  mol) was added to a degassed mixture of 5 mL of toluene and 4 mL of 2 M sodium carbonate aqueous solution. The mixture was vigorously stirred at  $85\text{--}90^\circ\text{C}$  for 48 h under a nitrogen atmosphere. After the mixture was cooled to room temperature, it was poured into a mixture of methanol and distilled water (10:1(v/v)) while being stirred. Orange polymer precipitate was collected on a filter. The recovered polymer was washed with methanol, water, and then methanol followed by Soxhlet extraction with methanol to remove oligomers and catalyst residue. The recovered yield was 73% (0.42 g).  $^1\text{H NMR}$  (300 MHz,  $\text{CDCl}_3$ , ppm):  $\delta$  7.86 (br, 2H, Ar-H),  $\delta$  7.68 (br, 4H, Ar-H),  $\delta$  7.44 (br, 5/95  $\times$  7H, Ar-H and  $-\text{CH}=\text{}$ ),  $\delta$  7.33 (m, 5/95  $\times$  4H, Ar-H),  $\delta$  7.19–7.21 (br, 5/95  $\times$  2H, Ar-H),  $\delta$  6.54–6.67 (m, 5/95  $\times$  3H, pyran-H and  $-\text{CH}=\text{}$ ),  $\delta$  2.42 (s, 5/95  $\times$  3H,  $-\text{CH}_3$ ),  $\delta$  2.12 (br, 4H,  $-\text{CH}_2(\text{CH}_2)_6\text{CH}_3$ ),  $\delta$  1.40 (s,  $-\text{C}(\text{CH}_3)_2-$ ),  $\delta$  1.14 (m, 20H,  $-\text{CH}_2(\text{CH}_2)_5\text{CH}_2\text{CH}_3$ ),  $\delta$  0.79–0.84 (br, 10H,  $-\text{CH}_2(\text{CH}_2)_5\text{CH}_2\text{CH}_3$ ). Anal. Calcd for  $\text{C}_{29}\text{H}_{38.95}\text{N}_{0.15}\text{O}_{0.05}$ : C, 89.20; H, 10.06; N, 0.54%. Found: C, 89.20; H, 9.89; N, 0.59%.

**PF-DCM 15.**<sup>31</sup> This polymer was prepared by the same manner as described above for the preparation of PF-DCM 05. A mixture of compounds **1** (0.283 g,  $5.16 \times 10^{-4}$  mol), **2** (0.474 g,  $7.37 \times 10^{-4}$  mol), and **5** (0.130 g,  $2.21 \times 10^{-4}$  mol) was polymerized in the presence of tetrakis(triphenylphosphine)palladium (8.5 mg,  $7.37 \times 10^{-6}$  mol). Polymer obtained was a red solid. The yield was 74% (0.43 g).  $^1\text{H NMR}$  (300 MHz,  $\text{CDCl}_3$ , ppm):  $\delta$  7.86 (br, 2H, Ar-H),  $\delta$  7.68 (br, 4H, Ar-H),  $\delta$  7.44 (br, 15/95  $\times$  7H, Ar-H and  $-\text{CH}=\text{}$ ),  $\delta$  7.33 (m, 15/95  $\times$  4H, Ar-H),  $\delta$  7.19–7.21 (br, 15/95  $\times$  2H, Ar-H),  $\delta$  6.54–6.67 (m, 15/95  $\times$  3H, pyran-H and  $-\text{CH}=\text{}$ ),  $\delta$  2.42 (s, 15/95  $\times$  3H,  $-\text{CH}_3$ ),  $\delta$  2.12 (br, 4H,  $-\text{CH}_2(\text{CH}_2)_6\text{CH}_3$ ),  $\delta$  1.40 (s,  $-\text{C}(\text{CH}_3)_2-$ ),  $\delta$  1.14 (m, 20H,  $-\text{CH}_2(\text{CH}_2)_5\text{CH}_2\text{CH}_3$ ),  $\delta$  0.79–0.84 (br, 10H,  $-\text{CH}_2(\text{CH}_2)_5\text{CH}_2\text{CH}_3$ ). Anal. Calcd for  $\text{C}_{29}\text{H}_{36.85}\text{N}_{0.45}\text{O}_{0.15}$ : C, 88.63; H, 9.42; N, 1.60%. Found: C, 87.97; H, 9.55; N, 1.50%.

**Poly[2,7-(9,9-dioctylfluorene)-alt-(1,4-phenylene- $\{\beta$ -(2-(4-dicyanomethylene-6-methyl-4H-pyran)-yl)styryl)imino-1,4-phenylene] (PF-DCM 50).**<sup>31</sup> A mixture of com-

Scheme 1. Synthetic Route to the Monomers



pounds **2** (0.474 g,  $7.37 \times 10^{-4}$  mol) and **5** (0.431 g,  $7.37 \times 10^{-4}$  mol) was polymerized in the presence of tetrakis(triphenylphosphine)palladium (8.5 mg,  $7.37 \times 10^{-6}$  mol) in the same manner as described above in the preparation of PF-DCM 05 and PF-DCM 15. PF-DCM 50 was a dark red solid. The yield was 70% (0.44 g).  $^1\text{H NMR}$  (300 MHz,  $\text{CDCl}_3$ , ppm):  $\delta$  7.86 (br, 2H, Ar-H),  $\delta$  7.68 (br, 4H, Ar-H),  $\delta$  7.44 (br, 7H, Ar-H and -CH=),  $\delta$  7.33 (m, 4H, Ar-H),  $\delta$  7.19–7.21 (br, 2H, Ar-H),  $\delta$  6.54–6.67 (m, 3H, pyran-H and -CH=),  $\delta$  2.42 (s, 3H, -CH<sub>3</sub>),  $\delta$  2.12 (br, 4H, -CH<sub>2</sub>(CH<sub>2</sub>)<sub>6</sub>CH<sub>3</sub>),  $\delta$  1.40 (s, -C(CH<sub>3</sub>)<sub>2</sub>-),  $\delta$  1.14 (m, 20H, -CH<sub>2</sub>(CH<sub>2</sub>)<sub>5</sub>CH<sub>2</sub>CH<sub>3</sub>),  $\delta$  0.79–0.84 (br, 10H, -CH<sub>2</sub>(CH<sub>2</sub>)<sub>5</sub>CH<sub>2</sub>CH<sub>3</sub>). Anal. Calcd for C<sub>29</sub>H<sub>29.5</sub>N<sub>1.5</sub>O<sub>0.5</sub>: C, 85.56; H, 7.31; N, 5.16%. Found: C, 85.19; H, 7.22; N, 5.07%.

**Measurements.**  $^1\text{H NMR}$  (300 MHz) and IR spectra were recorded on a Varian AM 300 spectrometer and on a Bomem MB FT-IR instrument, respectively. Elemental analyses were performed by the Center for Organic Reactions, Sogang University, Seoul, Korea, using an Eager 200 elemental analyzer. The purity of intermediates was confirmed by TLC on silica gel plates (MERCK, silica gel 60 F<sub>254</sub>) with a UV lamp (254 or 365 nm) and a visualization reagent. Molecular weights of polymers were determined by gel permeation chromatography (GPC; Waters) equipped with RI 2410 detector and Styragel HR52 column using polystyrene as standard. THF was employed as an eluent. Thermal properties were studied under a nitrogen atmosphere on a Mettler DSC 821 instrument. Thermogravimetric analysis (TGA) was performed under a nitrogen atmosphere at the heating/cooling rate of 10 °C/min on a Mettler TGA 50 thermogravimetric analyzer. The UV-vis spectra of polymers were obtained on a Hewlett-Packard 8452A diode array spectrophotometer. PL and EL spectra of polymers were acquired on an AMINCO-Bowman series 2 luminescence spectrometer. The current and luminescence intensity as a function of applied field were measured using an assembly consisting of PC-based dc power supply (Hewlett-Packard 6623A) and a digital multimeter (Hewlett-Packard 34401). A light power meter (Newport Instrument,

model 818-UV) was used to measure the device light output in microwatts. Luminance was measured by a Minolta LS-100 luminance meter. The thickness of polymers was determined by a TENCOR P-10 surface profiler. The redox properties of polymers were examined by cyclic voltammetry.<sup>32</sup> The polymer thin films were spin-coated on a platinum plate (1.5 cm<sup>2</sup>) using chlorobenzene as the solvent. The electrolyte solution employed was 0.10 M tetrabutylammonium tetrafluoroborate (Bu<sub>4</sub>NBF<sub>4</sub>) in acetonitrile. The Ag/AgNO<sub>3</sub> and Pt wire (600 μm in diameter) electrodes were utilized as reference and counter electrodes, respectively. The scan rate was 50 mV/s. For time-resolved photoluminescence (PL) analysis, all samples were excited by 315 nm pulses generated from a Raman shifter which was filled with 18 atm of methane gas and pumped by the fourth harmonic (266 nm, fwhm 20 ps, 10 Hz) of a hybrid mode-locked Nd:YAG laser (Continuum, Leopard D10). The PL kinetic profiles were obtained using a picosecond streak camera (Optronis, SCMU-ST-S20) connected with a spectrometer (CVI, DKSP240) and a CCD system (Optronis, SCRUS-SE-S). The observed PL decay curves were analyzed by a nonlinear least-squares iterative deconvolution method.

**Fabrication of LED Devices.** The devices have a structure of ITO/PEDOT (20 nm)/polymer (80–130 nm)/Li:Al (100 nm) or ITO/PEDOT (20 nm)/polymer (80–130 nm)/Alq<sub>3</sub> (3 nm)/Li:Al (100 nm). The ITO-coated glasses were cleaned as described earlier.<sup>33</sup> The conducting PEDOT layer (20 nm thick) was spin-coated onto the ITO-coated glasses in an argon atmosphere using a Laurell spin-coater. The emitting polymer layer then was spin-coated onto the PEDOT layer using the polymer solution in chlorobenzene. Finally, Li:Al alloy (100 nm, 2 wt % Li) electrodes were vacuum-deposited using a VPC-260 (ULVAC, Japan) vacuum coater and a CRTM-6000 thickness monitor (ULVAC, Japan) at a deposition rate of 5 Å/s onto the polymer layer at the pressure of  $2.0 \times 10^{-5}$  Torr. For bilayer devices, the Alq<sub>3</sub> layer was vacuum-deposited under a reduced pressure of  $2.0 \times 10^{-5}$  Torr onto the emitting polymer layer. Then, Li:Al alloy (100 nm) electrodes were deposited onto

Scheme 2. Synthesis of Polyfluorene Homo-(PF) and Copolymers (PF-DCMs)

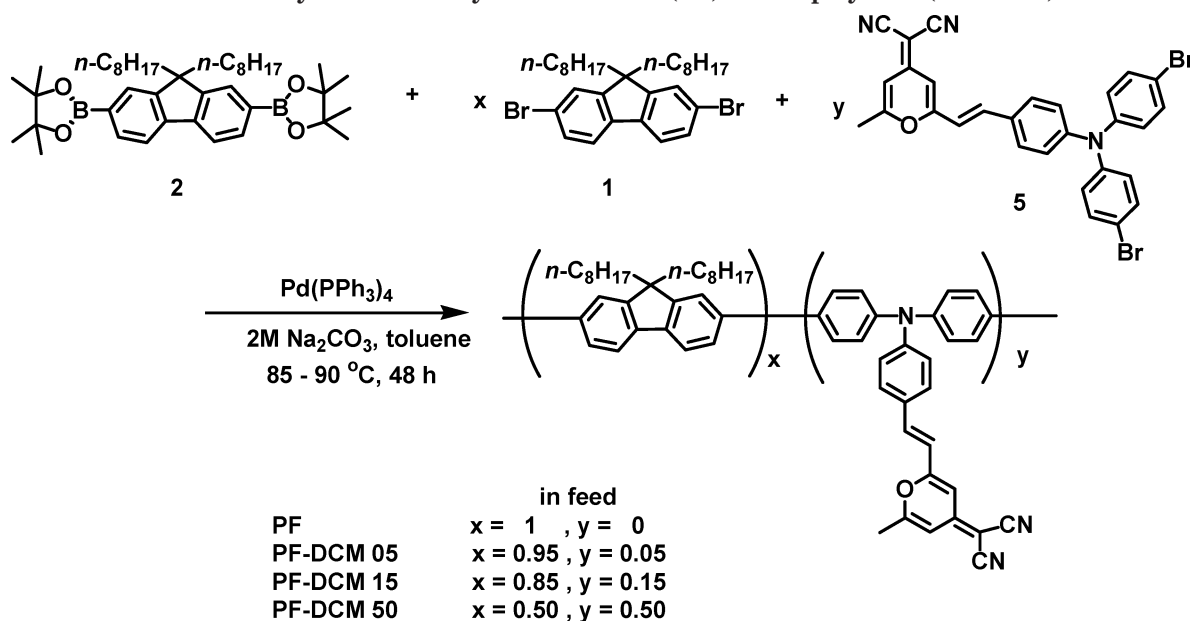


Table 1. General Properties of Polyfluorene Homo-(PF) and Copolymers (PF-DCMs)

	PF	PF-DCM 05	PF-DCM 15	PF-DCM 50
$\overline{M}_n^a$	11000	5600	5400	2300
$\overline{M}_w^a$	53000	14000	35000	7500
PDI	4.8	2.6	6.6	3.3
polymer yield (%) <sup>b</sup>	83	73	74	70
$y$ (%) <sup>c</sup>		4.5	12.8	50.0
$T_g$ (°C)	97	98		116
$T_d$ (°C) <sup>d</sup>	421	411	397	

<sup>a</sup> All values were obtained by GPC measurement with polystyrene as the calibration standard (eluent: tetrahydrofuran). <sup>b</sup> Recovered yields. <sup>c</sup> The  $y$  values were actual fractions of the DCM monomer unit in PF-DCM 05 and PF-DCM 15, as determined by <sup>1</sup>H NMR analysis. <sup>d</sup> The temperature revealing 5 wt % loss.

the Alq<sub>3</sub> layer under the same condition. The device efficiency and electroluminescence spectra were obtained by the same method as described in the literature.<sup>33</sup>

## Results and Discussion

**General Properties of Polymers.** Synthetic routes to the preparation of monomers and polymers can be found in Schemes 1 and 2. The monomers **1**, **2**, and **5** could be prepared, as shown in Scheme 1, using known synthetic reactions. Synthetic details were described in the Experimental Section. All the polymers, PF and the three copolymers, were prepared by the Suzuki coupling reaction<sup>31</sup> between 2,7-bis(4,4,5,5-tetramethyl-1,3,2-dioxaborolan-2-yl)-9,9-octylfluorene (**2**) and functionalized dibromoaromatic compounds (compounds **1** and **5**; refer to Scheme 1). They are soluble at room temperature in common organic solvents such as chloroform, tetrahydrofuran (THF), toluene, xylene, and chlorobenzene. Table 1 summarizes the polymerization results and general properties of the four polymers prepared in this investigation. The number-average molecular weight ( $\overline{M}_n$ ) of the polymers determined by GPC against polystyrene standard were  $11 \times 10^3$  ( $\overline{DP} = 28$ ) for PF,  $5.6 \times 10^3$  ( $\overline{DP} = 14$ ) for PF-DCM 05,  $5.4 \times 10^3$  ( $\overline{DP} = 14$ ) for PF-DCM 15, and  $2.3 \times 10^3$  ( $\overline{DP} = 6$ ) for PF-DCM 50. The eluent used was tetrahydrofuran (THF). The

polydispersity indices of the four polymers were estimated to be 4.8, 2.6, 6.6, and 3.3, respectively. It appears that the reactivity of compound **5**, which carries the DCM pendant, is much lower than that of compound **1**. Not only the actual contents (Table 1) of the monomer **5** unit incorporated into the copolymers are lower than in feed, but also molecular weights (Table 1) of copolymers are significantly reduced when compared with the molecular weight of PF. The actual compositions estimated by their <sup>1</sup>H NMR spectra of the two random copolymers (PF-DCM 05 and PF-DCM 15; refer to Scheme 2) prepared using the dibromo monomers (compound **1**:compound **5**) at feed compositions of  $m:n = 95:5.0$  and  $85:15$  in molar ratio are  $m:n = 95.5:4.5$  and  $87.2:12.8$ , respectively. Among the three copolymers, PF-DCM 50 is unique in that it is of alternating sequence of fluorene and DCM moieties, whereas the other two polymers are of random sequence. We note that the molecular weight of PF-DCM 50 is the lowest, which again suggests that DCM monomer **5** has a lower reactivity than monomer **1**.

Thermogravimetric analysis performed in a nitrogen atmosphere shows that thermal stability of the present polymers is fairly good. The temperature revealing 5 wt % loss decreased from 421 °C for PF to 379 °C for PF-DCM 50. The corresponding temperatures of the other two copolymers lie in between. The presence of the DCM units in the main chain of copolymers appears to lower the initial decomposition temperature. The glass transition temperatures ( $T_g$ s) of the polymers obtained by differential scanning calorimetry (DSC) are 97 °C for PF, 98 °C for PF-DCM 05, and 116 °C for PF-DCM 50. The relatively lower  $T_g$  values than expected for these polyaromatic polymers can be ascribed to the relatively low  $\overline{DP}$  and the presence of long alkyl groups in the fluorene units. The glass transition temperature of PF-DCM 15, however, could not be clearly identified on its thermogram. It appears that the presence of the polar DCM moieties in the copolymers increases the  $T_g$  value due to increased inter-chain interactions and bulkiness of the polar pendant groups, both of which are expected to reduce segmental motions.

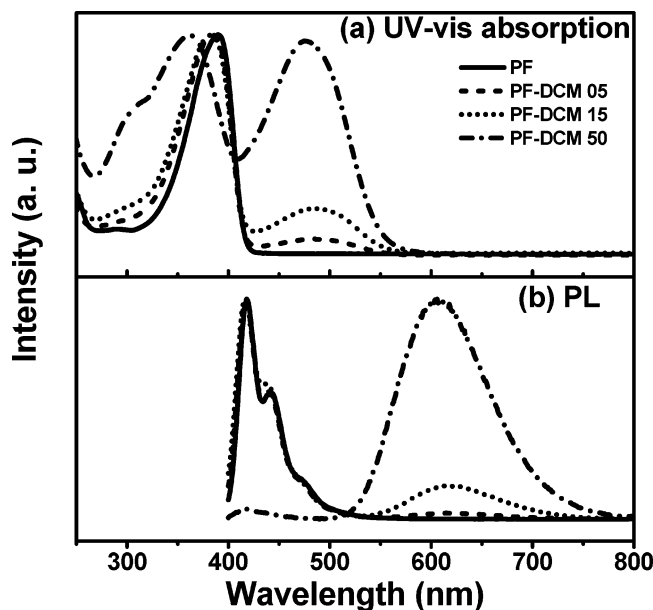


**Figure 1.** (a) UV-vis absorption and (b) photoluminescence (PL) spectra of the polymer solutions in chloroform ( $1.0 \times 10^{-5}$  M in repeating unit). All the PL spectra were recorded at the excitation wavelength of 370 nm, but the excitation wavelength of PF-DCM 50 was 361 nm.

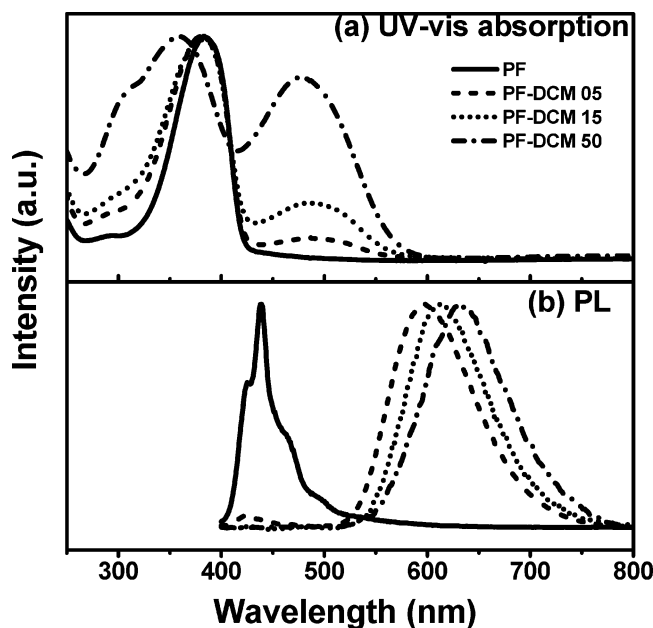


**Figure 2.** (a) UV-vis absorption and (b) photoluminescence (PL) spectra of the polymer films (100 nm thick). All the PL spectra were recorded at the excitation wavelength of 370 nm, but the excitation wavelength of PF-DCM 50 was 361 nm.

**Spectroscopic Properties.** Figures 1 and 2 display the absorption and photoluminescence (PL) spectra of the four polymers both in chloroform solution ( $1.0 \times 10^{-5}$  M in repeating unit) and in thin films (100 nm thick). According to the UV-vis absorption spectra shown in Figures 1 and 2, the homo- and copolymers display similar absorption spectral features both in chloroform solution and in the solid state. All the copolymers exhibit two major absorptions: one around 380 nm and the other over a longer wavelength region (400–550 nm). The first absorptions in the short wavelength region are originated from the  $\pi$ - $\pi^*$  transitions of main chain  $\pi$ -conjugated systems and the second from the

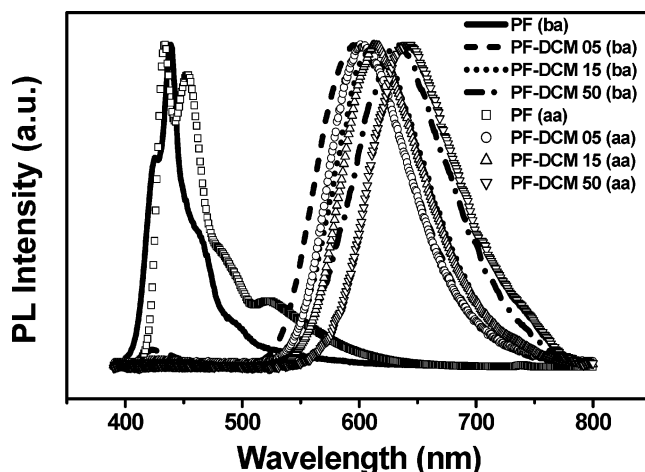


**Figure 3.** Emission spectra of PF, PF-DCM 05, PF-DCM 15, and PF-DCM 50 (100 nm thick) before and after annealing at 200 °C for 4 h. The designations “ba” and “aa” respectively refer to before annealing and after annealing at 200 °C for 4 h.

DCM unit.<sup>26,27</sup> As the fraction of the DCM moiety increases, the absorption maxima ( $\lambda_{\max}$ ) of the first peak are slightly blue-shifted because introduction of the triphenylamine segments of the DCM units into the main chains interrupts  $\pi$ -conjugation of the backbone. The  $\lambda_{\max}$  value of this peak moves from 390 nm for PF to 384 nm for PF-DCM 05, 383 nm for PF-DCM 15, and 361 nm for PF-DCM 50. The optical band gaps ( $E_g$ s) of the backbone  $\pi$ -systems estimated from the UV-vis absorption edges (435 nm for PF, 434 nm for PF-DCM 05, 431 nm for PF-DCM 15, and 415 nm for PF-DCM 50) are 2.85 (PF), 2.86 (PF-DCM 05), 2.88 (PF-DCM 15), and 2.99 eV (PF-DCM 50). Because the DCM moiety is incorporated into the PF main chain via the triphenylamine unit, it is not directly involved in the main chain conjugated structure, and the triphenylamine moiety acts as a generator of “kink” disorder. This kink effect leads to the increased  $E_g$  values of the copolymers with increasing the content of the DCM unit. At the same time, the absorption band position of the DCM moiety is rather independent of its content in the polymers due to the localization of its own  $\pi$ -system.

As shown in Figure 1, PL spectra of the copolymers obtained in chloroform solution at the excitation wavelength of 370 nm (excitation wavelength of PF-DCM 50 was 361 nm) display two characteristic emission bands at about 420 and 620 nm. Blue emission is considered to be arisen from the polyfluorenyl chromophoric segments disrupted by the DCM units as observed in the PL spectrum of the PF homopolymer, and the additional longer wavelength emission band is from the DCM units. However, the effect of incorporating the DCM units into the main chain on the luminescent properties is more dramatic in thin films. As shown in Figure 2, in all the copolymers no blue emission from the main chain, but only a longer wavelength reddish emission from the DCM units is observed. These results can be explained by easier exciton migration or energy transfer in the solid state from the polyfluorenyl segments to lower energy sites containing the DCM unit.<sup>22,23</sup> It also should be noted that the blue emission region by the polyfluorene segments overlaps significantly with the absorption region by the DCM moieties. In other words, there exist spectral overlaps for the copolymers, which is expected to favor energy transfer between the two

**Table 2. Optical Properties and Quantum Yield of Polyfluorene Homo-(PF) and Copolymers (PF-DCMs)**

polymers	$\lambda_{\max}$ (solution; $1.0 \times 10^{-5}$ M) <sup>a</sup>		$\lambda_{\max}$ (films) <sup>a</sup>		$E_g$ (eV) <sup>b</sup>	$\Phi_{\text{PL}}^c$
	abs	em	abs	em		
PF	390 (–)	418 (–)	383 (–)	418 (–)	2.85	1.00
PF-DCM 05	384 (485)	417 (598)	383 (484)	423 (598)	2.86	0.609
PF-DCM 15	383 (485)	417 (613)	383 (485)	– (613)	2.88	0.234
PF-DCM 50	361 (477)	420 (606)	361 (477)	– (632)	2.99	0.084

<sup>a</sup> The data in the parentheses are the absorption and emission wavelengths by the DCM unit. <sup>b</sup>  $E_g$  stands for the band-gap energy estimated from the onset wavelength of optical absorption. <sup>c</sup> Photoluminescence quantum yields in chloroform solution determined relative to coumarin 307.<sup>36b</sup>

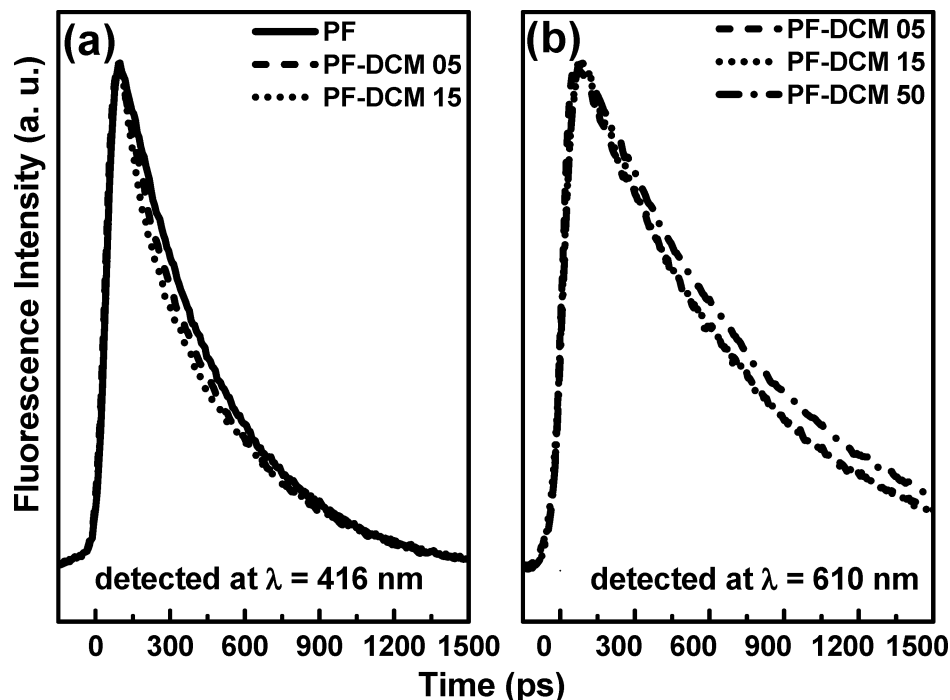


**Figure 4.** Time-resolved PL decay profiles of PF, PF-DCM 05, PF-DCM 15, and PF-DCM 50 in chloroform solution detected (a) at 416 nm and (b) detected at 610 nm with the excitation of 315 nm.

structural elements, and the emission maxima of the copolymers gradually shift to a longer wavelength from 598 nm for PF-DCM 05 to 632 nm for PF-DCM 50 as the DCM content increases.<sup>23b,c</sup>

We observed that the homopolymer, PF, shows an additional red-shifted emission<sup>8–15</sup> or a so-called green band at 530 nm when the polymer was subjected to a thermal annealing at temperatures above its  $T_g$ . However, all the present copolymers containing the DCM moieties display little change (Figure 3) in their emission even after annealing at 200 °C for 4 h. This annealing temperature is much higher than their respective  $T_g$ s. We believe that, as we alluded above, the presence of the triphenylamine units reduces the linearity of the main chain conformation and, thus, suppresses effective molecular packing. In Table 2, we present a summary of spectroscopic properties of all the polymers. According to the data given in the table, the PL quantum efficiency in solution decreases significantly with increasing the fraction of the DCM unit in copolymers. The luminescence efficiency decreases due to so-called “concentration quenching”,<sup>34</sup> owing to the formation of weakly emissive aggregates of intra- and/or intramolecular nature. There also are trapping or charge-transfer mechanisms proposed for such donor–acceptor type copolymer systems.<sup>23,35–37</sup>

**Time-Resolved PL Rise and Decay.** We have employed the time-resolved PL spectroscopy to obtain

further information on the energy transfer dynamics of the present copolymers. Figure 4a presents the PL decay profiles of PF, PF-DCM 05, and PF-DCM 15 in chloroform solution at the detection wavelength of 416 nm. We found that the samples did not show any detection wavelength dependence within the 416 nm band. Figure 4b exhibits the PL decay profiles of the copolymers (PF-DCM 05, PF-DCM 15, PF-DCM 50) in chloroform solution monitored at 610 nm where fluorescence is originated from the DCM moiety. The observed PL decay profiles were well fitted to the single- or double-exponential function. In Table 3, the fitted values for the rise and decay components of the exponential functions are summarized for the polymer samples in chloroform solution. Figure 4b and Table 3 clearly demonstrate that the copolymers revealed rise time in contrast to the homopolymer, PF, that did not so.

As shown in Table 3, the PL decay of the homopolymer (PF) exhibits a single-exponential decay with the lifetime of 370 ps. On the other hand, the copolymers of PF-DCM 05 and PF-DCM 15 follow the double-exponential decay consisting of a fast and a slow component at the detection wavelength of 416 nm, which is the emission wavelength from the polyfluorene moiety. The fast decay components (38–50 ps) at 416 nm show a good correlation with the rise components (32–47 ps) of the copolymers at the detection wavelength of 610 nm, which corresponds to the emission

**Table 3. PL Lifetime and Relative Amplitude of the Polymers in Chloroform Solution**

sample	$\lambda$ (nm)	rise $\tau_1$ (ps) <sup>a</sup>	decay $\tau_2$ (ps)/ $A_2$ <sup>a</sup>	decay $\tau_3$ (ps)/ $A_3$ <sup>a</sup>
PF	416			370 ( $\pm 5$ )
PF-DCM 05	416		45 ( $\pm 5$ )/0.17 ( $\pm 0.02$ )	372 ( $\pm 5$ )/0.83 ( $\pm 0.02$ )
	610	35 ( $\pm 3$ )		1320 ( $\pm 10$ )
PF-DCM 15	416		43 ( $\pm 5$ )/0.39 ( $\pm 0.02$ )	395 ( $\pm 5$ )/0.61 ( $\pm 0.02$ )
	610	43 ( $\pm 3$ )		1300 ( $\pm 10$ )
PF-DCM 50	610	44 ( $\pm 3$ )		1450 ( $\pm 10$ )

<sup>a</sup>  $I(t) = -A_1 \exp(-t/\tau_1) + A_2 \exp(-t/\tau_2) + A_3 \exp(-t/\tau_3)$ , where  $I(t)$ ,  $A$ , and  $\tau$  are the time-dependent fluorescence intensity, relative amplitude, and lifetime, respectively. The excitation wavelength for all decays was 315 nm.

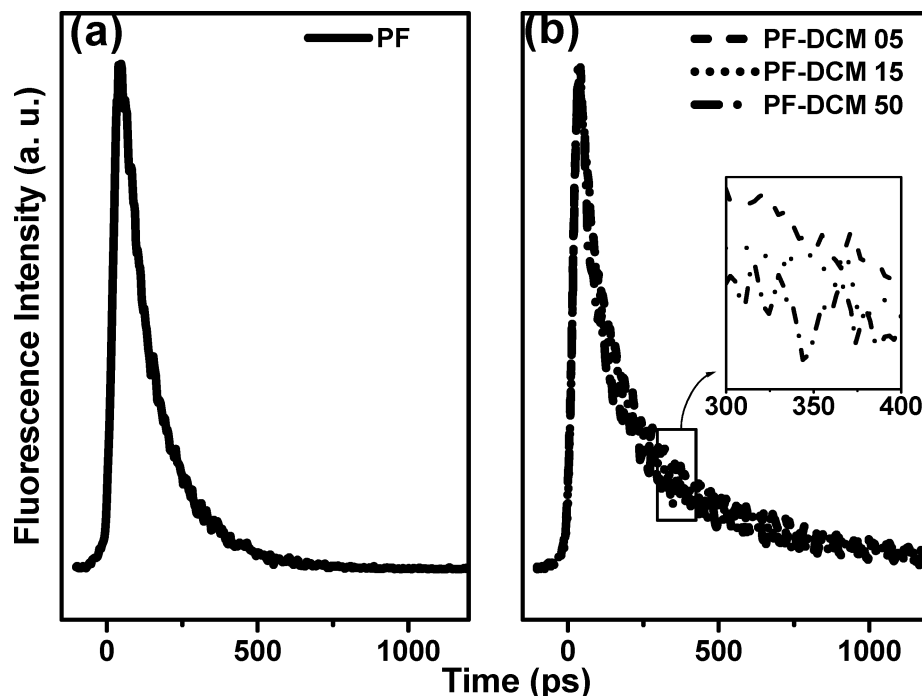


**Figure 5.** Time-resolved PL decay profiles of PF, PF-DCM 05, PF-DCM 15, and PF-DCM 50 films detected at 439, 608, 623, and 640 nm with the excitation of 315 nm.

wavelength of the DCM moiety. Therefore, it can be suggested that the  $S_1$  state energy transfer occurs at the time scale of  $\sim 45$  ps from the polyfluorene parts to the DCM moieties in chloroform solution. The slow components (372, 395 ps) of PF-DCM 05 and PF-DCM 15 detected at 416 nm are attributed to the intrinsic decays of the polyfluorene parts in the backbone without energy transfer, which is the same as the decay profile of the homopolymer, PF. And it is noted that the amplitudes of the slower decay components are much greater than those of the faster decay components. The other slow components of 1.3–1.4 ns at the 610 nm detection are responsible for the intrinsic lifetimes of the DCM moiety.

Figure 5a,b displays the PL decay profiles of the homopolymer (PF) and the copolymers in thin films (100 nm thick). As shown in Table 4, the homopolymer film exhibits a single-exponential decay with the lifetime of  $\sim 110$  ps at the detection wavelength of 439 nm, and the copolymer films (PF-DCM 05, PF-DCM 15, PF-DCM 50) follow the double-exponential decay consisting of the fast components (45–62 ps) and the slow components (330–426 ps) at the detection wavelengths of 608, 623, and 640 nm, respectively. All the films experienced a slight detection wavelength dependence of the lifetime within the 10–40 ps range, which is ascribed to the structural inhomogeneities existing in the films. The samples in film exhibit much shorter PL lifetimes compared with those in chloroform solution. Such

**Table 4. PL Lifetime and Relative Amplitude of the Polymer Films**

sample	$\lambda$ (nm)	decay $\tau_1$ (ps)/ $A_1$ <sup>a</sup>	decay $\tau_2$ (ps)/ $A_2$ <sup>a</sup>
PF	439	110 ( $\pm 5$ )	
PF-DCM 05	608	56 ( $\pm 5$ )/0.64 ( $\pm 0.02$ )	409 ( $\pm 10$ )/0.36 ( $\pm 0.02$ )
PF-DCM 15	623	57 ( $\pm 5$ )/0.70 ( $\pm 0.02$ )	416 ( $\pm 10$ )/0.30 ( $\pm 0.02$ )
PF-DCM 50	640	50 ( $\pm 5$ )/0.69 ( $\pm 0.02$ )	340 ( $\pm 10$ )/0.31 ( $\pm 0.02$ )

<sup>a</sup>  $I(t) = A_1 \exp(-t/\tau_1) + A_2 \exp(-t/\tau_2)$ , where  $I(t)$ ,  $A$ , and  $\tau$  are the time-dependent fluorescence intensity, relative amplitude, and lifetime, respectively. The excitation wavelength for all decays was 315 nm.

shorter PL lifetimes of films are known to be due to the various fast nonradiative decay processes such as exciton trapping by defect sites via enhanced interchain interactions.<sup>38</sup> In particular, the rise components of the copolymer films at  $\sim 620$  nm responsible for the DCM emission are not observed, when compared with the emissions from their solutions, within our detection resolution limit of  $\sim 10$  ps in the utilized collection window. It implies that, in the film states, the  $S_1$  state energy-transfer process occurs much faster than the process in the solution. This must be due to the much better contact between polyfluorene parts and DCM moieties in solid films than in solutions. In addition, there is an interesting point to be noted: the fast and slow decay time constants of films are not much different from those of solutions, but the amplitudes of the fast decay components are much greater than those of

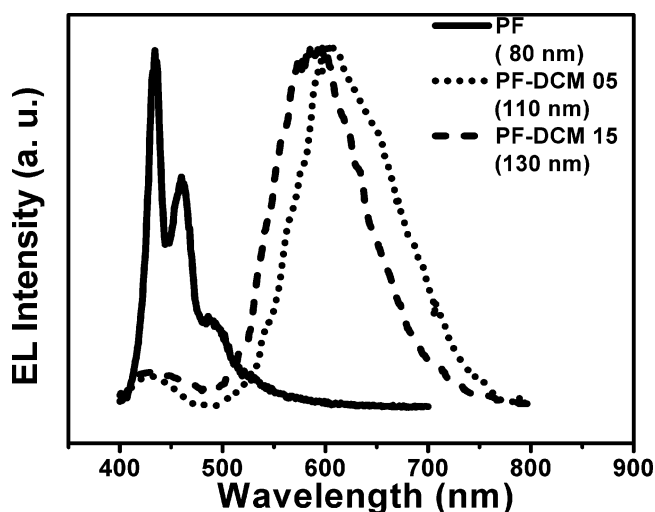
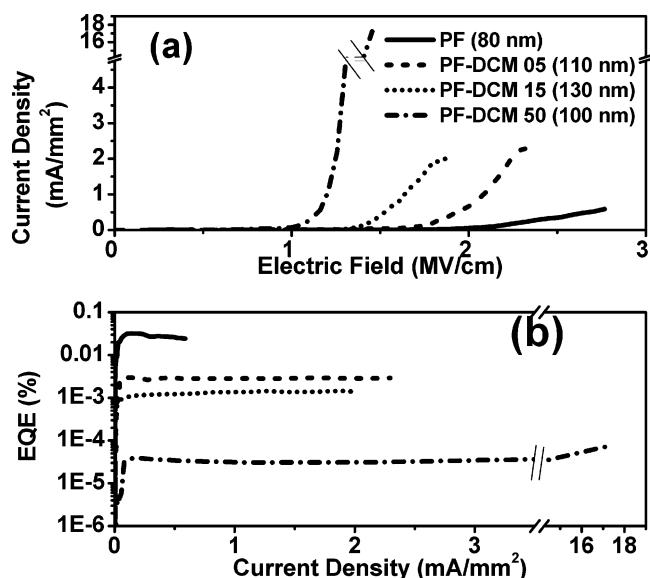
**Table 5. Band-Gap Characteristics of the Polymers As Determined from CV Data and UV-Vis Absorption Edges**

sample	band gap (eV)	oxidation onset (V) vs Ag/AgNO <sub>3</sub> (0.10 M)	HOMO (eV)	LUMO (eV)
PF	2.85	1.39	5.79	2.94
PF-DCM 05	2.86	1.37	5.77	2.91
PF-DCM 15	2.88	1.32	5.72	2.84
PF-DCM 50	2.99	0.89	5.29	2.30

the slow decay components, which is in contrast to the case of solutions. This must be one of the important factors causing lower PL efficiencies of solid films when compared with solution.

**Electrochemical Properties.** The redox behaviors of the polymers were investigated by cyclic voltammetry (CV).<sup>32</sup> From CV,<sup>32</sup> we could determine the ionization potentials (IPs), i.e., the HOMO levels, of the polymer backbones. The oxidative onset potential was taken as the IP value. The LUMO levels then were estimated from the HOMO levels and optical band gaps ( $E_{gs}$ ) of the backbones determined from the absorption edges of their UV-vis absorption spectra. The work function of ITO was taken to be 4.8 eV.<sup>39</sup> The results are summarized in Table 5. The HOMO level of the main chain of the polymers steadily decreases from 5.79 eV for PF to 5.29 eV for PF-DCM 50 with increasing the fraction of DCM moiety.<sup>40</sup> As to the LUMO level, it also decreases from 2.94 eV for PF to 2.84 eV for PF-DCM 15 with increasing the content of the DCM unit followed by a decrease to 2.30 eV with a further increase in the DCM content in PF-DCM 50. The latter significant decrease, however, should be more of the result of the alternating sequence of the two repeating units in PF-DCM 50.

**Electrical and Electroluminescence Properties of LED Devices.** Electroluminescence of the LED devices constructed with the four polymers was studied in detail. The device configuration was ITO/PEDOT (20 nm)/polymer (80–130 nm)/Li:Al (100 nm). The electroluminescence (EL) spectra of the devices are presented in Figure 6. The EL spectra of polymers are very similar to the corresponding PL spectra of their thin films, which indicates that the same luminescence mechanism is involved in both EL and PL. Unfortunately, we could not obtain the EL spectrum of PF-DCM 50 due to its low light output and poor devices stability. Figure 7 shows the  $I$ - $V$  characteristics of the four devices. The turn-on electric field decreases from 1.95 MV/cm for the PF device to 0.94 MV/cm for the PF-DCM 50 device. The other two copolymers exhibit the turn-on electric field of 1.60 and 1.22 MV/cm, respectively, with the value being lower for the copolymer containing a higher level of the DCM unit. Comparison of the values of turn-on electric field of the devices with the HOMO levels (Table 5) of the corresponding polymers leads to the conclusion that the smaller the difference between the work function of the ITO anode and the HOMO level of a polymer, the lower the turn-on electric field becomes. This, in turn, implies that easier hole injection from the anode controls the turn-on electric field of the present devices, which should hold true only when the major carrier is the positive hole. Moreover, we observed that the external quantum efficiency of the devices dramatically decreased with increasing the DCM content. It decreased from about  $3 \times 10^{-2}\%$  for the blue-emitter PF to  $4 \times 10^{-5}\%$  for the red-emitter PF-DCM 50. From the comparison of the values of external quantum efficiency of the devices with the

**Figure 6.** Electroluminescence spectra of single-layer devices of ITO/PEDOT (20 nm)/Polymer/Li:Al (100 nm).**Figure 7.** (a) Dependence of current density on electrical field and (b) external quantum efficiencies of single-layer LED devices.

LUMO levels (Table 5) of the corresponding polymers, we reach a conclusion that the larger the difference between the work function of lithium metal (2.9 eV)<sup>41</sup> and the LUMO level of a polymer, the lower the external quantum efficiency. This indicates that the energy barrier for electron injection from the cathode controls the external quantum efficiency of the present devices, which is also consistent with above statement that the major carrier is hole and the minor carrier is electron. Therefore, imbalance in the injection of the positive holes and electrons leads to the diminished efficiencies. It is also well-known<sup>42</sup> that balance in the mobility of the opposite carriers is important for improved efficiencies of EL devices. We, however, presently do not have information on the carriers' mobility of these polymers. In addition, fluorescence quenching induced by the charge-transfer mechanism may be applicable to EL of the present copolymers consisting of electron-donor and -acceptor segments.

When we inserted a very thin layer (3 nm thick) of Alq<sub>3</sub>,<sup>43</sup> the well-known electron injecting and transporting materials, between the emitting polymer layers and



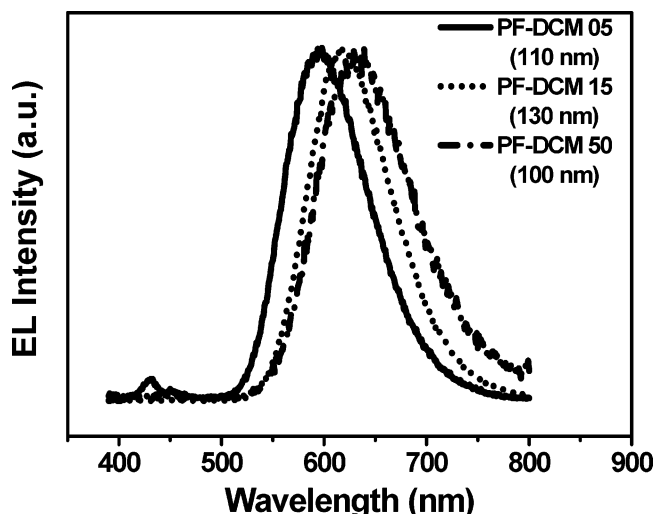


**Figure 8.** Electroluminescence spectra of bilayer devices: ITO/PEDOT (20 nm)/Polymer/Alq<sub>3</sub> (3 nm)/Li:Al (100 nm).

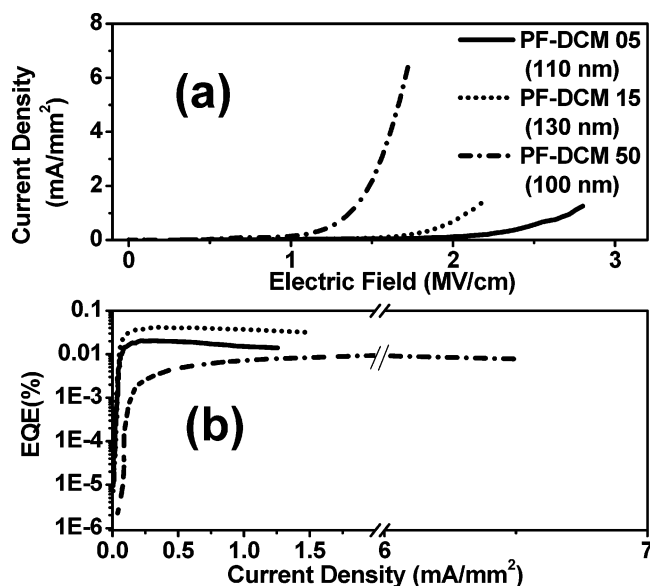


**Figure 9.** (a) Dependence of current density on electrical field and (b) external quantum efficiencies of the bilayer LED devices.

the cathode (device configuration: ITO/PEDOT(20 nm)/polymer(100–130 nm)/Alq<sub>3</sub>(3 nm)/Li:Al(100 nm)), we obtained EL spectra (Figure 8) very similar to their PL spectra with no trace of emission from the Alq<sub>3</sub> layer. This indicates that the excitons are effectively formed in the emitting polymer layer through combination between the injected positive holes into the polymer and electrons transported through the Alq<sub>3</sub> layer from the cathode. Figure 9a shows the *I*–*V* characteristics of the bilayer devices. The turn-on electric field of the bilayer device was almost same as that of single-layer device. However, the efficiency (Figure 9b) of the bilayer devices was  $2.1 \times 10^{-2}\%$  for PF-DCM 05,  $4.2 \times 10^{-2}\%$  for PF-DCM 15, and  $1.0 \times 10^{-2}\%$  for PF-DCM 50. Maximum brightness of the bilayer devices was 65 cd/m<sup>2</sup> at 2.82 MV/cm (1.28 mA/mm<sup>2</sup>) for PF-DCM 05, 70 cd/m<sup>2</sup> at 2.23 MV/cm (1.56 mA/mm<sup>2</sup>) for PF-DCM 15, and 60 cd/m<sup>2</sup> at 1.80 MV/cm (6.86 mA/mm<sup>2</sup>) for PF-DCM 50. These values are much higher than those (Figure 7b) of single-layer devices. Especially, the increase for the PF-DCM 50 device was more than 2 orders of magnitude. This implies that an efficient electron injection and

transport by the presence of the Alq<sub>3</sub> layer leads to an improved electron–hole recombination and thus to an improved EL efficiency.

## Conclusion

We have described the synthesis and luminescence properties of a series of new polyfluorene copolymers bearing DCM moieties as pendants. The polymers were prepared by the well-known palladium-catalyzed Suzuki coupling reaction. They show good solubility at room temperature in common organic solvents such as chloroform, tetrahydrofuran (THF), toluene, xylene, and chlorobenzene. They exhibit moderately high glass transition temperatures (>97 °C) and also good thermal stability. UV–vis absorption spectra of three copolymers showed two major absorptions by the main chain (380 nm) and also by the DCM units (485 nm). Although in chloroform solution the copolymers displayed simultaneous PL emissions at 420 and 610 nm from both structural components, in the solid state they exhibited a quite dramatic change in emission spectra. The copolymers showed only a long wavelength emission at 620 nm originated from the DCM moieties with no trace of emission from the main chain. We also observed that light emission of the LED devices fabricated with them was solely from the segments containing the low-band-gap structure, i.e., the DCM moiety. This is interpreted by an efficient energy transfer or exciton migration from the polyfluorene main chain to the low-band-gap trap sites or the acceptor DCM moieties. This energy transfer could be unequivocally supported by a time-resolved PL decay study. The PL efficiencies of the copolymers in solution decreased significantly with increasing the fraction of DCM unit, which is attributed to concentration quenching at high DCM content. Copolymerization with the DCM monomer suppresses an undesired long wavelength emission and leads to a stabilized emission from these copolymers due to fast energy transfer from the fluorene moiety to the DCM unit. The triphenylamine moiety of the DCM comonomer unit incorporated into the main chain disrupts the linear structure of the conjugated polyfluorene backbone, which, in turn, increases the band-gap energy of the copolymers. This leads to an enhanced hole injection from the anode, but to a diminished electron injection from the cathode to the emitting layer. EL efficiency of PLED devices dramatically decreases with increasing the content of the DCM moiety. When we fabricated bilayer devices inserting a thin layer of electron transporting Alq<sub>3</sub> layer between the emitting polymer layer and the cathode, we observed significantly improved EL efficiencies, which is conjectured to be due to improved injection of the electrons to the active layer. This investigation provides us with excellent examples of polymers that could demonstrate facile excited energy transfer from one structural part to the other.

**Acknowledgment.** This work was supported by the Korea Science and Engineering Foundation through CRM of Korea University. C.H.C. and S.-H.J. were the Brain Korea 21 Fellow supported by the Ministry of Education and Human Resources, Korea. Y.-R.K. thanks to National Research Laboratory grant (Grant M1-0302-00-0027) for financial support.

## References and Notes

- (1) Burroughes, J. H.; Bradley, D. D. C.; Brown, A. R.; Marks, R. N.; MacKay, K.; Friend, R. H.; Burn, P. L.; Holmes, A. B. *Nature (London)* **1990**, *347*, 539.

- (2) (a) Kraft, A.; Grimaldi, A. C.; Holmes, A. B. *Angew. Chem., Int. Ed.* **1998**, *37*, 402. (b) Denton, F. R., III; Lahti, P. M. In *Photonic Polymer Systems—Fundamentals, Methods, and Application*; Wise, D. L., Cooper, T. M., Wnek, G. E., Gresser, J. D., Trantolo, D. J., Eds.; Marcel Dekker: New York, 1998; Chapter 3. (c) Yang, Y.; Heeger, A. J. *Nature (London)* **1994**, *372*, 344. (d) Yang, Z.; Sokolik, I.; Karasz, F. E. *Macromolecules* **1993**, *26*, 1188. (e) Yoon, C. B.; Moon, K. J.; Shim, H. K. *Macromolecules* **1996**, *29*, 5754. (f) Hsieh, B. R.; Antoniadis, H.; Bland, D. C.; Feld, W. A. *Adv. Mater.* **1995**, *7*, 36. (g) Jiang, X. Z.; Register, R. A.; Killeen, K. A.; Thompson, M. E.; Pschenitzka, F.; Sturm, J. C. *Chem. Mater.* **2000**, *12*, 2542. (h) Wang, Y. Z.; Sun, R. G.; Meghdadi, F.; Leising, G.; Epstein, A. J. *Appl. Phys. Lett.* **1999**, *74*, 3613.
- (3) Salaneck, W. P.; Lundstorm, I.; Ranby, B. *Conjugated Polymers and Related Materials*; Oxford University Press: Oxford, 1993; pp 65–169.
- (4) Braun, D.; Heeger, A. J. *Appl. Phys. Lett.* **1991**, *58*, 1982.
- (5) Friend, R. H.; Gymer, R. W.; Holmes, A. B.; Burroughes, J. H.; Marks, R. N.; Taliani, C.; Bradley, D. D. C.; Dos Santos, D. A.; Bredas, J. L.; Logdlund, M.; Salaneck, W. R. *Nature (London)* **1999**, *397*, 121.
- (6) (a) Chung, S.-J.; Kwon, K. Y.; Lee, S. W.; Jin, J.-I.; Lee, C. H.; Lee, C. E.; Park, Y. *Adv. Mater.* **1998**, *10*, 1112. (b) Chung, S.-J.; Jin, J.-I.; Lee, C. H.; Lee, C. E. *Adv. Mater.* **1998**, *10*, 684–688. (c) Kim, K.; Hong, Y.-R.; Lee, S.-W.; Jin, J.-I.; Park, Y.; Sohn, B.-H.; Kim, W.-H.; Park, J.-K. *J. Mater. Chem.* **2001**, *11*, 3023. (d) Lee, D. W.; Kwon, K. Y.; Jin, J.-I.; Park, Y.; Kim, Y. R.; Hwang, I. W. *Chem. Mater.* **2001**, *13*, 565. (e) Kang, H. S.; Kim, K. H.; Kim, M. S.; Park, K. T.; Kim, K. M.; Lee, T. H.; Lee, C. Y.; Joo, J.; Lee, D. W.; Hong, Y. R.; Kim, K.; Lee, G. J.; Jin, J.-I. *Synth. Met.* **2002**, *130*, 279. (f) Park, J. H.; Kim, K.; Hong, Y. R.; Jin, J. I.; Sohn, B. H. *Macromol. Symp.* **2004**, *212*, 51. (g) Cha, S. W.; Jin, J.-I. *Synth. Met.* **2004**, *143*, 97.
- (7) Scherf, U.; List, E. J. W. *Adv. Mater.* **2002**, *14*, 477.
- (8) (a) Pei, Q.; Yang, Y. *J. Am. Chem. Soc.* **1996**, *118*, 7416. (b) Yang, Y.; Pei, Q. *J. Appl. Phys.* **1997**, *81*, 3294.
- (9) (a) Chen, X.; Liao, J. I.; Liang, Y.; Ahmed, M. O.; Tseng, H.-E.; Chen, S.-A. *J. Am. Chem. Soc.* **2003**, *125*, 636. (b) Rathore, R.; Abdelwahed, S. H.; Guzei, I. A. *J. Am. Chem. Soc.* **2003**, *125*, 8729.
- (10) Inaoka, S.; Advincula, R. *Macromolecules* **2002**, *35*, 2426.
- (11) Grell, M.; Long, X.; Bradley, D. D. C.; Inbasekaran, M.; Woo, E. P. *Adv. Mater.* **1997**, *9*, 798.
- (12) (a) Virgili, T.; Lidzey, D. G.; Bradley, D. D. C. *Synth. Met.* **2000**, *111–112*, 203. (b) Kreyenschmidt, M.; Klarner, G.; Fuhrer, T.; Ashenhurst, J.; Karg, S.; Chen, W. D.; Lee, V. Y.; Scott, J. C.; Miller, R. D. *Macromolecules* **1998**, *31*, 1099.
- (13) Xia, C.; Advincula, R. C. *Macromolecules* **2001**, *34*, 5854.
- (14) Lee, J.-I.; Klarner, G.; Chen, J. P.; Scott, J. C.; Miller, R. D. *SPIE Int. Soc. Opt. Eng.* **1999**, *3623*, 2.
- (15) Miteva, T.; Meisel, A.; Knoll, W.; Nothofer, H. G.; Scherf, U.; Muller, D. C.; Meerholz, K.; Yasuda, A.; Neher, D. *Adv. Mater.* **2001**, *13*, 565.
- (16) (a) Lemmer, U.; Heun, S.; Mahrt, R. R.; Scherf, U.; Hopmeier, M.; Siegner, U.; Göbel, E. O.; Müllen, K.; Bäessler, H. *Chem. Phys. Lett.* **1995**, *240*, 371. (b) Pannozzo, S.; Vial, J.-C.; Kervalla, Y.; Stéphan, O. *J. Appl. Phys.* **1995**, *240*, 373. (c) Herz, L. M.; Phillips, R. T. *Phys. Rev. B* **2000**, *61*, 13691. (d) Zeng, G.; Yu, W. L.; Chua, S. J.; Huang, W. *Macromolecules* **2002**, *35*, 6907.
- (17) (a) Gong, X.; Iyer, P. K.; Moses, D.; Bazan, G. C.; Heeger, A. J.; Xiao, S. S. *Adv. Funct. Mater.* **2003**, *13*, 325. (b) Gaal, M.; List, E. J. W.; Scherf, U. *Macromolecules* **2003**, *36*, 4236. (c) Jacob, J.; Crimsdale, A. C.; Müllen, K. *Macromolecules* **2003**, *36*, 8240. (d) List, E. J. W.; Günter, R.; Scandiucci de Freitas, P.; Scherf, U. *Adv. Mater.* **2002**, *14*, 374.
- (18) Klarner, G.; Davey, M. H.; Chen, W. D.; Miller, R. D. *Adv. Mater.* **1998**, *10*, 993.
- (19) Jenekhe, S. A.; Osaheni, J. A. *Science* **1994**, *265*, 765.
- (20) (a) Buckley, A. R.; Rahn, M. D.; Hill, J.; Cabanillas-Gonzales, J.; Fox, A. M.; Bradley, D. D. C. *Chem. Phys. Lett.* **2001**, *339*, 331. (b) O'Brien, D. F.; Giebeler, C.; Fletcher, R. B.; Cadby, A. J.; Palilis, L. C.; Lidzey, D. G.; Lane, P. A.; Bradley, D. D. C.; Blau, W. *Synth. Met.* **2001**, *116*, 379. (c) (a) Gong, X.; Ostrowski, J. C.; Bazan, G. C.; Moses, D.; Heeger, A. J.; Liu, M. S.; Jen, K.-Y. *Adv. Funct. Mater.* **2003**, *13*, 45.
- (21) Inbasekaran, M.; Wu, W.; Woo, E. P. U.S. Patent 5777070, 1997.
- (22) Klarner, G.; Lee, J.-I.; Davey, M. H.; Miller, R. D. *Adv. Mater.* **1999**, *11*, 115.
- (23) (a) Lee, J.-I.; Klarner, G.; Davey, M. H.; Miller, R. D. *Synth. Met.* **1999**, *102*, 1087. (b) Cho, N. S.; Hwang, D.-H.; Lee, J.-I.; Jung, B.-J.; Shim, H.-K. *Macromolecules* **2002**, *35*, 1224. (c) Huang, J.; Niu, Y.; Yang, W.; Mo, Y.; Yuan, M.; Cao, Y. *Macromolecules* **2002**, *35*, 6080. (d) Lee, J.-I.; Zyung, Y.; Miller, R. D.; Kim, Y. H.; Jeoung, S. C.; Kim, D. J. *J. Mater. Chem.* **2000**, *10*, 1547.
- (24) Hou, Q.; Zhou, Q.; Zhang, Y.; Yang, W.; Yang, R.; Cao, Y. *Macromolecules* **2004**, *37*, 6299.
- (25) (a) Chen, C. H.; Klubek, K. P.; Shi, J. U. S. Patent 5908581, 1999. (b) Chen, C. H.; Klubek, K. P.; Shi, J. U. S. Patent 5935720, 1999.
- (26) (a) Chen, C. H.; Shi, J.; Tang, C. W. *Macromol. Symp.* **1997**, *125*, 1. (b) Jung, B.-J.; Yoon, C.-B.; Shim, H.-K.; Do, L.-M.; Zyung, T. *Adv. Funct. Mater.* **2001**, *11*, 430. (c) Kim, J. H.; Lee, H. *Chem. Mater.* **2002**, *14*, 2270.
- (27) Peng, Q.; Lu, Z.-Y.; Huang, Y.; Xie, M.-G.; Han, S.-H.; Peng, J.-B.; Cao, Y. *Macromolecules* **2004**, *37*, 260.
- (28) Armarego, W. L. F.; Perrin, D. D. *Purification of Laboratory Chemicals*, 4th ed.; Butterworth Heinemann Press: Woburn, MA, 1996; p 334.
- (29) Ranger, M.; Rondeau, D.; Leclerc, M. *Macromolecules* **1997**, *30*, 7686.
- (30) Woods, L. L. *J. Am. Chem. Soc.* **1958**, *80*, 1440.
- (31) Miyaura, N.; Suzuki, A. *Chem. Rev.* **1995**, *95*, 2457.
- (32) (a) Helbig, M.; Horhold, H.-H. *Makromol. Chem.* **1993**, *194*, 1607. (b) Jamietz, M.; Bradley, D. D. C.; Grell, M.; Giebeler, C.; Inbasekaran, M.; Woo, E. P. *Appl. Phys. Lett.* **1998**, *73*, 2453. (c) Cervini, R.; Li, X.-C.; Spencer, G. W. C.; Holmes, A. B.; Moratti, S. C.; Friend, R. H. *Synth. Met.* **1997**, *84*, 359.
- (33) Braun, D.; Heeger, A. J. *Appl. Phys. Lett.* **1991**, *58*, 1982.
- (34) (a) Morgado, J.; Cacialli, F.; Friend, R. H.; Iqbal, R.; Yahioglu, G.; Milgrom, L. R.; Moratti, S. C.; Holmes, A. B. *Chem. Phys. Lett.* **2000**, *325*, 552. (b) Tang, C. W.; VanSlyke, S. A.; Chen, C. H. *J. Appl. Phys.* **1989**, *65*, 3610.
- (35) Demas, J. N.; Crosby, G. A. *J. Phys. Chem.* **1971**, *75*, 991.
- (36) (a) Hila, S. J.; Ramin, J.; Yitzhak, T. *Angew. Chem., Int. Ed.* **1999**, *38*, 2722. (b) Fery-forgues, S.; Lavabre, D. *J. Chem. Educ.* **1999**, *76*, 1260.
- (37) Chen, Z. K.; Huang, W.; Wang, L. H.; Kang, E. T.; Chen, B. T.; Lee, C. S.; Lee, S. T. *Macromolecules* **2000**, *33*, 9015.
- (38) Samuel, I. D. W.; Crystall, B.; Rumbles, G.; Burn, P. L.; Holmes, A. B.; Friend, R. H. *Chem. Phys. Lett.* **1993**, *213*, 472.
- (39) Park, Y.; Choong, V.; Gao, Y.; Heish, B. R.; Tang, C. W. *Appl. Phys. Lett.* **1996**, *68*, 2699.
- (40) (a) Redecker, M.; Bradley, D. D. C.; Inbasekaran, M.; Wu, W. W.; Woo, E. P. *Adv. Mater.* **1999**, *11*, 241. (b) Liu, B.; Huang, W. *Thin Solid Films* **2002**, *417*, 206. (c) Redecker, M.; Bradley, D. D. C.; Inbasekaran, M.; Woo, E. P. *Appl. Phys. Lett.* **1998**, *73*, 1565.
- (41) Lide, D. R. *Handbook of Chemistry and Physics*, 75th ed.; CRC Press: London, 1994; Chapter 12, p 114.
- (42) (a) Baigent, D. R.; Greenham, N. C.; Gruner, J.; Marks, R. N.; Friend, R. H.; Moratti, S. C.; Holmes, A. B. *Synth. Met.* **1994**, *67*, 3. (b) Heeger, A. J.; Parker, I. D.; Yang, Y. *Synth. Met.* **1994**, *67*, 23. (c) Jang, J. W.; Lee, C. E.; Lee, D. W.; Jin, J.-I. *Solid State Commun.* **2004**, *130*, 265.
- (43) (a) Wu, C. C.; Chun, J. K. M.; Burrows, P. E.; Sturm, J. C. *Appl. Phys. Lett.* **1995**, *66*, 653. (b) Hosokawa, H.; Tokailin, H.; Kusumoto, T. *Appl. Phys. Lett.* **1992**, *60*, 1220. (c) Kelper, R. G.; Beeson, P. M.; Jacobs, S. J.; Anderson, R. A.; Sinclair, M. B.; Valencia, V. S.; Cahill, P. *Appl. Phys. Lett.* **1995**, *66*, 3618. (d) Kim, K.; Lee, D. W.; Jin, J.-I. *Synth. Met.* **2000**, *114*, 49.